Electrical Engineering (2022) 104:4239–4254
https://doi.org/10.1007/s00202-022-01616-2

ORIGINAL PAPER

The effects of non-standard lightning impulse on electrical insulation: a review

Pradipta Ghosh[1] · **Arup Kumar Das**[2] · **Sovan Dalai**[2] · **Saibal Chatterjee**[1]

Received: 5 February 2022 / Accepted: 16 July 2022 / Published online: 9 August 2022

Abstract

Equipment installed in a power system network has to tolerate impulse overvoltage throughout its life span. Lightning impulses are one of the primary reasons of this overvoltage. Hence, insulation of the power equipment is designed and tested with standard lightning impulse. However, in reality, various complex, oscillatory non-standard lightning impulse waveforms exist in natural lightning impulses. Therefore, for the better design of insulation of the power equipment, identification of the non-standard lightning impulse waveform is essential. This article presents a comprehensive review of the effects of non-standard lightning impulse voltage on the insulation of power equipment. This article will help to classify the non-standard lightning impulse waveforms and identify the parameters, generation circuit, and analysis of non-standard lightning impulse waveforms till the present day. Hence, the information presented in the article can be helpful for the insulation design of the power equipment.

Keywords Breakdown voltage · Electric stress · Insulation · Non-standard lightning impulse waveforms

1 Introduction

With the rapid development of the electric power grid, many new and costly pieces of equipment are installed in the power system network. To achieve a reliable and uninterrupted power supply, the equipment must be healthy. However, the equipment is constantly exposed to lightning impulse voltages. Lightning is a natural phenomenon. The protective devices (exp- lightning arresters) are connected to power equipment to bypass lightning impulses. However, the protective devices may not work correctly against the lightning strokes due to their intermittent properties [1, 2]. So, the power equipment installed in the power system network should have the proper insulation strength to withstand the lightning impulse voltage.

According to IS-2071-1 [3] and IEC 60,060-1 [4], standard lightning impulse (SLI) voltage is a unidirectional voltage with no appreciable oscillation. It increases quickly to the peak value and decreases much slowly to zero. The standard waveshape of lightning impulse was first mentioned by IEC in 1962 [5]. The standard waveshape can be defined as (1.2×50) µs wave. It signifies that the time to reach the peak value of the waveshape is 1.2 µs, whereas the time to reach half of the peak value is 50 µs. In Fig. 1, the waveshape of (1.2×50) µs has been depicted. In Fig. 1, "t_1" indicates the time to attain the peak value from the origin, whereas "t_2" denotes the time to reach half of the peak value from the origin, respectively. It is pertinent to mention here that the permissible deviation in a SLI wave is less than ± 3% of the peak value, ± 30% of the front time, and ± 20% of the tail time. A lightning impulse voltage waveform (LIVW) is called a full lightning impulse voltage waveshape when no puncture or flashover occurs. The front time of lightning impulses must be limited up to 20 µs [3, 4]. Lightning impulse could be from a range of kHz to MHz. So, there is a rapid increment in stress within a short time duration, affecting the insulation system of power equipment. Therefore, power equipment are tested by keeping in mind that they have to withstand standard lightning impulse (SLI), and similarly, their insulation has been designed. However, in real life, the non-standard lightning impulse waveforms (NSLIW) are present in natural lightning impulse [6–13]. So, for a

✉ Pradipta Ghosh
pradipta.ghosh14@gmail.com

1 Department of Electrical and Electronics Engineering, National Institute of Technology Mizoram, Aizawl, Mizoram, India

2 Department of Electrical Engineering, Jadavpur University, Kolkata, India

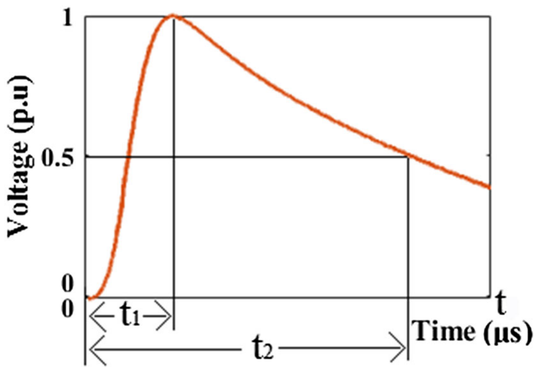

Fig. 1 The waveshape of lightning impulse voltage waveform [3]

longer life span, reliable operation, and uninterrupted power supply, the insulation system of power equipment must be designed, considering NSLIW. Hence, the identification and characteristics of the non-standard lightning impulses voltage waveforms (NSLIVW) must be appropriately known.

This review article presents a comprehensive study on the generation, classification, and the effects of non-standard lightning impulses over the electrical insulation throughout the past century. The paper is structured as follows: Categorization of NSLIW is described in section-2, while section-2 is subcategorized into two parts. In the first part (A), classification based on the length of the impulse waveform is shown, and the second part (B) illustrates the variation based on the nature of the impulse waveform. Variable parameters of NSLI depending on the nature of the impulse waveform are presented in section-3. Section-4 consists of the practical generation circuit of NSLI. It is subdivided into two sections. The generation circuit of (A, B, C-1, and D) waveforms is discussed in the first subsection, and the generation circuit of the rest two waveforms (C-2 and E) are described in the second subsection. The state-of-the-art study on the NSLIVW is analyzed in section-5. In section-6, the effect of NSLIVW on the insulation of HV equipment is discussed, and afterward, conclusions and references will end the article.

2 Categorization of non-standard lightning impulse waveforms

Lightning impulse waveform differs from these expected values [3, 4], then it is considered NSLIW. Previous research [6–13] shows that the waveshape of natural lightning impulse waves differs quite a bit from the SLIW [(1.2 × 50) µs]. Depending upon a variable tail time (length of wave tail time) and the nature of waveforms, NSLIW may be classified mainly into two sections.

2.1 Classification based on the tail time

An impulse waveform is called a "short-tail lightning impulse" if the tail time of the waveform is less than the standard value (50 µs), whereas the impulse waveform is known as "long-tail lightning impulse" when the tail time of the waveform is greater than the standard value (50 µs). Over the last few decades, researchers have been interested in short- and long-tail lightning impulses. In Table 1, the synopsis of the previous research based on impulse waveform variable tail time has been presented. The effect of variable tail time on different insulation systems (air, oil, cable, etc.) has also been mentioned in Table 1.

2.2 Classification based on the nature of lightning impulse waveform

According to several types of research, the nature of lightning impulse waveform in transmission lines and cable systems may differ from standard lightning impulse (SLI). The nature or waveshape of the lightning impulse waveform depends on the design and layout of the substation, the arrangement of equipment, and various states of switches [7, 11, 39–42]. Depending on the experimental investigation, Okabe et al. in [39–42] described five types of NSLIW as follows:

i. "A-waveform" or "single-pulse waveform": As the name suggests, the wave consists of a single pulse. The waveshape of the A-waveform is totally different from rest of the non-standard impulse waveforms. It neither has any steeper wavefront nor is oscillatory in nature. In Fig. 2, waveshape of A-waveform has been presented. [11, 39, 41, 42].
ii. "B-waveform" or "Pulse-in wavefront waveform": This type of waveform may be described with an abrupt growth in the wavefront region and a flat wave tail region. In Fig. 3, the waveshape of the B-waveform has been shown. The B-waveform occurrence depends upon the length between the surge arrester and the gas-insulated switchgear (GIS) terminal [7, 11, 42].
iii. C-waveform: This type of waveform is defined as the "damped-oscillation waveform (single-frequency oscillation waveform)." There are many resonance points present in a substation because of various series and parallel equipment. C-waveform is generated when the oscillations between the substation's incoming bushing and the GIS end become commanding. The "C-waveform" is also known as "C1-waveform." If restriking happens within the substation, a higher-frequency surge with a damped-oscillation waveform is created. It is also recognized as "C2-waveform." In C2-waveform, two different high frequencies can be observed [11, 39,

Table 1 Details study on short- and long-tail lightning impulse

Ref. No	Year	Authors	Impulse waveforms used	Some important outcome
[14]	1934	AIEE Committee	i. (1 × 5) µs ii. (1.5 × 40) µs	The minimum impulse flashover voltage for insulators and gaps were explained. From the experimental results it was observed that the impulse flashover voltages for string of insulators [(4 disks of 10″ with 5.75″ spacing) and (8 disks of 10″ with 5.75″ spacing)] were obtained by applying (1 × 5) µs and (1.5 × 40) µs impulse voltages, respectively
[15]	1984	Carrus et al	i. (1.05 × 47) µs ii. (1.15 × 5.7) µs iii. (1.2 × 4.7) µs iv. (1.25 × 3.9) µs v. (1.4 × 3.3) µs vi. (0.95 × 52) µs vii. (1.15 × 6) µs viii. (1.2 × 5) µs ix. (1.35 × 4) µs x. (1.35 × 53) µs xi. (1 × 6) µs xii. (1 × 5) µs xiii. (0.95 × 4) µs	By adequately applying internal and external resistances, the production of very short-tail lightning impulse (4–6) µs is achieved. However, it has been observed that the efficiency of the generated impulse voltages dropped to about 15%
[16]	1987	Burrage et al	i. (10 × 175 ± 75) ns ii. (100 × 500 ± 100) ns iii. (500 × 1000 ± 200) ns iv. (1.2 × 50) µs	The winding voltage distribution of a shell and core type transformer was calculated after the application of low voltage impulses
[17]	1989	A. Carrus	i. (0.87 × 3.7) µs ii. (0.88 × 4) µs iii. (0.91 × 4.5) µs iv. (0.93 × 4.8) µs v. (0.96 × 5) µs vi. (0.84 × 2.8) µs vii. (0.86 × 3.4) µs viii. (0.91 × 4.9) µs ix. (0.94 × 6.35) µs x. (1.2 × 5) µs	A new type of Marx circuit was designed for the generation of short-tailed lightning impulses. It was found that a short-tail impulse was generated for a constant wave tail resistance by only adding high valued series inductance to the circuit
[18]	1989	Lux et al	Rise-time: i. 65 ns ii. 90 ns iii. 100 ns iv. 300 ns	The breakdown voltage (BDV) of XLPE (cross-linked polyethylene) cable insulation is proportional to the rise-time of steep front short duration (SFSD) impulses. However, by monitoring breakdown strength, the degradation of XLPE insulated cables cannot be appropriately observed. The experimental investigation also revealed no remarkable change in dissipation factor of the XLPE cable insulation due to repeated SFSD impulse applications
[19]	1989	J. H. Shaw	i. (1.2 × 50) µs ii. (100 × 500) ns iii. (10 × 150) ns	The experimental set of apparatus validated for a steep front impulse to be well organized, sensible, and dependable for continuous keeping data and preparing printouts while required. That experimental set may be useful for superior resolution
[20]	1989	Aoshima et al	i. (1 × 70) µs ii. (2 × 70) µs iii. [(1.1–1.7) × (2.8–40)] µs	It was observed that the 50% flashover voltage of insulator is inversely proportional to the tail time of the impulse waveform. The experimental investigation also revealed that the 50% flashover voltage of the insulator is proportional to relative humidity during the application of short-tailed lightning impulse (STLI). The flashover possibility of insulator is higher during application STLI with respect to SLI
[21]	1990	Miller et al	i. (60 × 240) ns ii. (125 × 240) ns	The steep front short duration (SFSD) impulses can be generated by using a coaxial cable with a Marx type impulse generator. From the experimental results it was revealed that the minimum breakdown voltage (V_{min}) porcelain suspension insulators were 1.5 times more for SFSD pulses with respect to standard lightning impulses (SLI) and porcelain, elastomers, and heat-shrink terminators (2–3) times more voltage withstand capacity for SFSD impulses with respect to SLI

Table 1 (continued)

Ref. No	Year	Authors	Impulse waveforms used	Some important outcome
[22]	1990	Grzybowski et al	(65 ns × 5 µs)	For short front pulses, the insulator critical flashover (CFO) voltage was 1.5 to 2 times higher with respect to SLIs (1.2 × 50) µs
[23]	1996	H. Motoyama	i. (1 × 4) µs-0.4 m gap ii. [(1.2–1.4) × (3.2–3.7)] µs–(1–3) m gap	The leader breakdown procedure was explained, and the leader onset state was illustrated by mathematical expressions. An advanced model on breakdown occurrence was presented. It was noticed that the model precisely recognized the breakdown operation and v-t characteristics with the STLI and SLI than earlier models
[24]	1999	Carrus et al	i. (1.2 × 50) µs ii. (1.2 × 4) µs	It was observed from the experimental results that the higher possibility of (up to 30%) flashover for STLI [(1.2 × 4) µs] than SLI. It was also observed that the insulators of 3 kV DC traction lines take a longer time to flashover for STLI than SLI
[25]	2003	Venkatesan et al	(1.2 × 50) µs	The "multiresolution signal decomposition (MSD)" and "mathematical curve fitting (MCF)" approaches were applied to determine the mean curve and evaluate the lightning impulse parameters. For the initial parameters in the converged solution, MSD has a higher impact than the MCF technique
[26]	2004	Grzybowski et al	(60 × 200) ns	As the necessary voltage for breakdown is higher for the longer air gap, the BDV for the combination of wooden cross arm and insulator is much higher. The consolidated insulation system (wooden cross arm and insulator) responds better to SFSD than SLI
[27]	2004	Grzybowski et al	(60 ns × 200 ns)	The system CFO voltage is higher for SFSD than SLI while having the combination of wooden cross-arm and insulator in the insulation system. Total electrical strength is improved by a wooden cross arm
[28]	2007	Ancajima et al	i. (1.2 × 50) µs ii. (1.2 × 4) µs	For longer air gap distances and positive polarity, v-t characteristic is higher for STLI with respect to SLI
[29]	2014	Braz et al	i. (1.2 × 4) µs ii. (1.2 × 10) µs iii. (1.2 × 50) µs	For STLI [(1.2 × 4) µs, (1.2 × 10) µs] and SLI of both polarities, the v-t characteristics curve was obtained for the 15 kV pin porcelain insulator. The method suggested by Ancajima et al. [30] to forecast the breakdown characteristics of distribution type insulators under NSLI was satisfactory
[31]	2014	Lantharthong et al	Current waveform: i. (0.25 × 100) µs ii. (10 × 100) µs iii. (5 × 350) µs iv. (10 × 350) µs	The rise-time of impulse current has more impact to the back flashover rate (BFOR) and pole top voltage with respect to tail time. Due to the negative reflection coefficient, the BFOR and pole top voltage becomes higher with respect to SFSD impulse waveforms
[32]	2014	Wang et al	i. (1.05 × 51.5) µs-110 kV ii. (1.28 × 54.5) µs-220 kV iii. (1.56 × 49.2) µs-500 kV B. Short-Tail Impulse: i. (1.1 × 6.5) µs-110 kV ii. (1.1 × 15.7) µs-220 kV iii. (1.45 × 11) µs-500 kV	The leader development model proposed by the authors recognized the breakdown procedure of the insulator more precisely. It was observed that the variables from the experiments can be applied to protect porcelain and composite insulators of (110–500) kV transmission lines

Table 1 (continued)

Ref. No	Year	Authors	Impulse waveforms used	Some important outcome
[33]	2014	Yuan et al	(1.5 × 15) µs	From the experiments, it was identified that the 50% BDV for STLI [(1.5 × 15) µs] is (25–30) % higher with respect to SLI. It was observed that with respect to positive-polarity, negative polarity STLI's 50% BDV is 5% more
[34]	2016	Sima et al	i. (1.2 × 50) µs ii. (5.4 × 50) µs iii. (6.4 × 50) µs iv. (11 × 50) µs v. (14.4 × 50) µs vi. (15.6 × 50) µs vii. (16.7 × 50) µs viii. (20 × 50) µs ix. (26 × 50) µs	The v–t characteristics curve must be lower for SFSD waveform with respect to longer wavefront time. While applying a negative impulse to oil-impregnated paper (OIP) insulation in COMSOL Multiphysics software, it was observed that negative current is dependent on wavefront time and positive current has higher sensitivity on wave tail time. The experimental result obtained that the negative current has a higher peak value with respect to positive polarity
[35]	2018	Yamamoto et al	Current impulse (10 × 350) µs	The authors have designed a long wave tail impulse current generator, which will effectively generate a waveform that is very adjacent to the existing winter lightning current waveform
[36]	2018	Xiao et al	(0.5 × 5) µs	The back flashover voltage goes down for polluted insulators with respect to clean insulators. The power frequency voltage rarely influenced the impulse flashover attributes of contaminated insulators. As per the tracks of flashover of contaminated insulators, different outcomes were observed for STLI with respect to AC voltage
[37]	2018	Zhao et al	(0.6 × 8.6) µs	While computing the breakdown time, the streamer onset time must be anticipated. The streamer onset time should be considered when the breakdown time is calculated, particularly when the composite insulator strings have the grading rings
[38]	2018	Han et al	i. (1.2 × 50) µs ii. (1 × 10) µs iii. (0.84 × 50) µs	The 50% breakdown voltage ($U_{50\%}$) is (20–40) % more for STLI with respect to those for SLI. For the time of breakdown of more than 3 µs, then primary dissimilarity was observed in the v-t characteristics of the impulse waveform. Because of the shielding deficiency or back flashover that occurs on the transmission lines, the impact of the impulse waveform and the insulator substances must be considered while the computation of lightning protection behavior

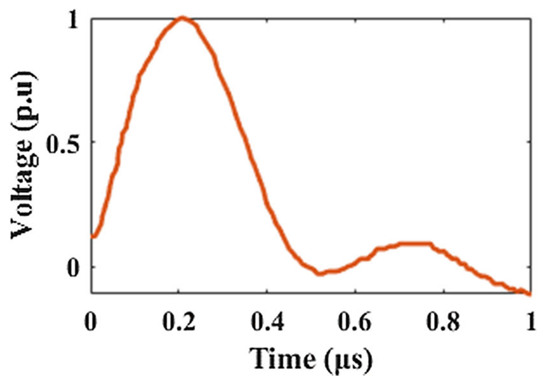

Fig. 2 The waveshape of single-pulse or A-waveform [39]

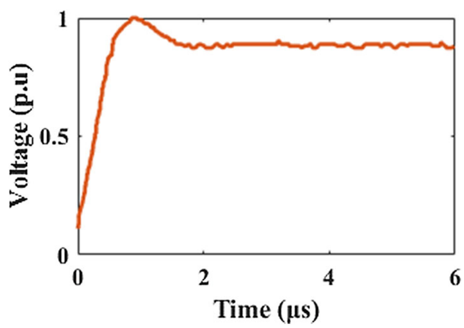

Fig. 3 The waveshape of pulse-in or B-waveform [42]

40]. "C1-waveform" and "C2-waveform" are shown in Figs. 4 and 5, respectively.

iv. "D-waveform" or "Rising-oscillation waveform": In this type of waveform, the magnitude of second peak is greater than the first peak and the magnitude reduces thereafter [11, 39, 41]. This type of waveform is generated because of the superposition of delayed surges, which appears due to frequent reflections between flashover points and bushings. In Fig. 6, a graphical representation of "D-waveform" has been illustrated.

v. "E-waveform" or "double-frequency oscillation waveform": This damped oscillating impulse waveform is generated due to superposition of two crucial frequencies. The reciprocating impulses on GIS primary bus and shorter branches are of comparatively low frequencies and high frequencies, respectively. The superposition of these two different frequency impulse waveforms generates the "double-frequency oscillation waveform" or "E-waveform." E-waveform is shown in Fig. 7 [39].

The characteristics of the non-standard lightning impulse waveforms would be appropriately identified by knowing the parameters of the NSLIWs. These parameters, i.e., rise-time, tail time, damping time constants, frequency ranges, and peak

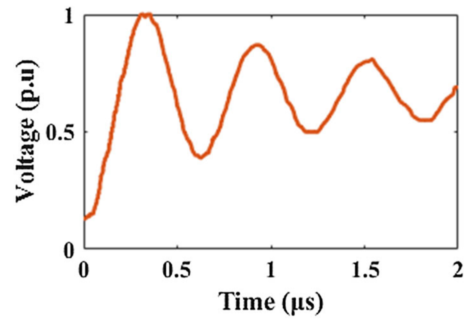

Fig. 4 C-1 waveform [39]

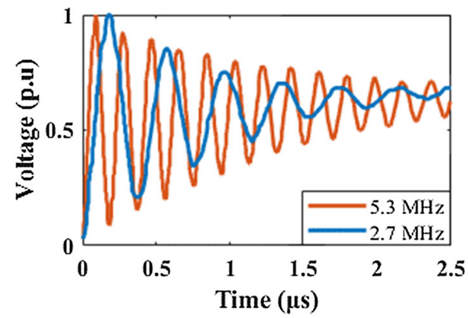

Fig. 5 C-2 waveform [39]

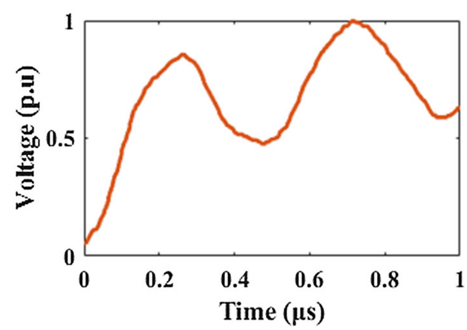

Fig. 6 The waveform of rising-oscillation or D-waveform [39]

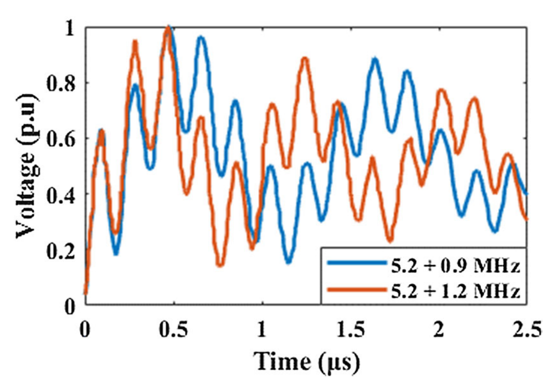

Fig. 7 Waveshape of double frequency oscillation or E waveform [39]

Table 2 Variables of test waveshapes [39]

Waveshapes		Span of variables	
		Wavefront section	Wave tail section
SLI		T_{front}: 1.2 µs	T_{tail}: 50 µs
E		Low "f": 0.9–1.2 MHz	τ_d: 4.2–46.4 µs
		High "f": 4.0–5.2 MHz	
D		T_{front}: 0.25–0.94 µs	E_1/E_2: 0.65–1.0
C	C_1	T_{front}: 0.2–1.2 µs	E_2/E_1: 0.75–0.9
	C_2	f: 0.85–5.3 MHz	τ_d: 0.83–32.6 µs
B		T_{front}: 0.26–0.98 µs	E_2/E_1: 0.73–0.88
A		T_{front}: 0.2–0.85 µs	T_{tail}: 0.26–1.65 µs

voltage magnitudes of first few peaks, are essential for identifying the characteristics of the NSLIWs. The details about those parameters are described in the next section.

3 Parameters of non-standard lightning impulse voltage waveform

In this section, the variable parameters of both standard and non-standard lightning impulse waveforms depending on voltage and time are illustrated in Table 2. These varying parameters of NSLIW were obtained by Okabe et al. [39] after the analysis of their experimental work. In Table 2, the rise-time for the first peak of the non-standard impulse waveform is specified as the "T_{front}." The wave tail time is denoted as "T_{tail}." The damping time constant is represented as "τ_d." Frequency is marked as "f." A negative polarity voltage was implemented as the negative polarity voltage is observed to be much more stressful in the matter of insulation concerning the lightning surge period [39]. E_1 and E_2 are the voltages recognized as the first and second peaks of the impulse wave, respectively. For B-waveform, E_2 is the voltage of the steady-state section of the impulse waveform, and the voltage magnitude of the third peak of the C-1 impulse waveform is noted as E_3.

From this table it was observed that the impulse frequency was always in MHz range irrespective of the type of impulse waveform. The rise-time of the NSLIWs (A, B, C-1, and D) varied in the span of (0.2–1.2) µs, and for oscillating NSLIWs (C-2 and E), rise-time varied from (0.1886–1.176) µs. From the (E_1/E_2) ratio of the D-waveform, it was noticed that the voltage magnitude of the second peak is greater than the first peak, as it was stated in previous section. The generation of NSLIWs is necessary to know the effects of NSLIW on the electrical insulation and different test objectives. For that purpose, the generation circuit of NSLIW is essential.

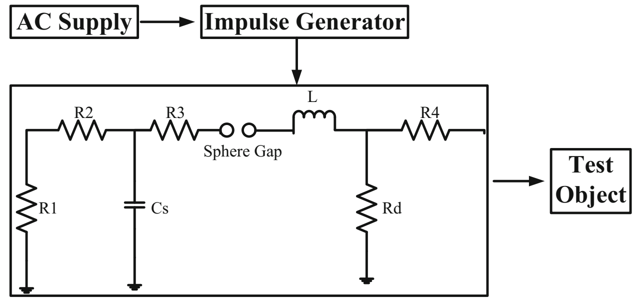

Fig. 8 Schematic diagram of A, B, C-1, and D waveform generation [42]

The generating circuits of NSLIW are discussed in the next section.

4 Generation of non-standard lightning impulse waveshape

The standard lightning impulses are practically generated with the help of an impulse voltage generator. The modifications are needed to the impulse voltage generator to generate non-standard lightning impulse voltage. In this section, the generation circuit is explained. The generation circuit for single-frequency NSLIW and double-frequency NSLIW are discussed in two subsections.

4.1 Generation of A, B, C-1, and D waveform:

The generation circuit of NSLIW (A, B, C-1, and D) is described here. Okabe et al. explained the NSLIWs generating circuit (A, B, C-1, and D) in [7, 42]. There the impulse voltage was generated with the help of an impulse voltage generator. The fundamental block diagram of the circuit elements used for the generation of NSLIWs is displayed in Fig. 8. The series–parallel combination of resistance (*R*), inductance (*L*), and capacitances (*C*) was connected through a sphere-gap. Then NSLIWs were generated by adequately controlling the series–parallel combination of RLC parameters. After the generation of NSLIW (A, B, C-1, and D), those were fed to the test objective. Here charging capacitance is denoted as C_S and the inductance of the connecting wires is represented as L.

The fundamental of the working circuit has been described as follows: Across a series connected air gap the impulse voltage was generated. The LC oscillation was produced between the charging capacitance (C_S) and test objective through inductance L. As a result, single-frequency oscillation impulse waveform (C-1) was produced. For the generation of the rising-oscillation (D) waveform, a lower value of resistance R_2 was added to the C-1 waveshape generation circuit (as shown in Fig. 8). The circuit's time constant would be changed, and the oscillation will be increased. Hence, the voltage magnitude of the second peak will be more with respect to the first peak of the impulse voltage and D-waveform was generated.

It is essential to present (R_3 + R_4) to damp the oscillation of the C-1 waveform (in Fig. 8) for the generation of the B waveform. So, the oscillation ended within in one cycle only and steady-state took place in wave tail region. To generate an A waveform, the damping in the impulse wave tail region must be increased. It was done by decreasing the value of Rd. As a consequence, single-pulse waveform (A waveform) was produced. The charging capacitance (C_S) primarily regulates the rise-time of NSLIW on the power supply end. The EMTP software is used to identify the specified circuit constants needed to generate the above four types of NSLIWs. To establish the reliability of the generated waveforms, these parameters of the generation circuit must be designed indeed.

4.2 Generation of C-2 and E waveform:

This section discussed the primary generation circuit for C-2 and E non-standard lightning waveforms. Okabe et al. had explained the generating circuit of NSLIWs (C-2 and E) [7–9, 39, 42–54]. Like in the previous section, test circuits were first created in EMTP. Evaluation, investigation, and generation of different voltage levels, gap between test electrode, settings of impulse generator, and circuit elements were done through EMTP. After that, the experimental setup was prepared. As explained in the previous section, the C-2 waveshape is developed fundamentally similar to the C-1 waveshape. The fundamental block diagram of the test circuit is illustrated in Fig. 9.

The experimental setup circuit was verified with a 300 kV single-phase supply. As the C-2 waveshape's frequency range is higher, one inductor was inserted after the series gap in the circuit. One high-valued resistor was added before the series gap to control the damping of the oscillating waves. For the generation of E-waveform, an inductance was put after the series gap to generate a high-frequency oscillation, and another inductance was placed before the series gap. A capacitance following the series gap to develop low-frequency oscillation. Hence, by the superposition of two high frequency oscillation, double-frequency oscillation waveform (E- waveform) was produced.

5 State-of-the-art study on non-standard lightning impulse voltage waveshape

Various researches have tried to illuminate different areas of non-standard lightning impulse waveform (NSLIW). In this paper, an attempt has been made to study and analyze the research outcomes (breakdown, limitations, etc.) of NSLIW.

A. R. Jones in 1954 [55] experimented with (1.5 × 40) µs LIW over standard insulation to check the precession of the integration method. It was discovered that the rod-gaps were much more superior to traditional solid insulation in terms of impulse flashover. Estimation of constants from the mathematical expressions was one of the biggest drawbacks of the integration method. In 1985, Shindo and Suzuki proposed an advanced model to recognize the predischarge current and computation of breakdown v-t characteristic [56]. The model was verified by using four types of LIs [(1.5 × 50) µs, (1.5 × 40) µs, (2.5 × 53) µs, and (2.4 × 9.6) µs] over rod–plane gap (0.25–5 m), rod–rod gaps (0.3–1.5 m) successfully. Li et al. in [57] experimented with two NSLIW [(0. 2 × 60) µs, (1. 25 × 60) µs] over the coaxial cylindrical gap and rod-sphere gaps in different dielectrics (exp- SF_6 & air mix, N_2, etc.). From the experiment, it was observed that 50% BDV of rod-sphere gap and coaxial cylindrical gap in the mixture of dry air, SF_6 and N_2 is inversely proportional to the sharpness of the wavefront region.

In 1988, M. Darveniza and A. E. Vlastos suggested to utilize the integration method to estimate the impulse strength of the NSLIW [58]. It was noted that by using this integration method, significant results were obtained irrespective of the class, type, and configurations of insulation. The results showed that the precision limits varied [(± 5) to (± 15)]%, depending on the gaseous insulation configurations. The same authors prescribed a theoretical concept with a generalized integration method to predict impulse v-t characteristics for NSLIW [59]. In 1989, Pigini et al. experimented the impulse breakdown for several gap distances (rod–rod gap, rod–plane gap) with a few NSLIWs [(1.6 × 50) µs, (1.6 × 18) µs, (0.7 × 25) µs, (0.5 × 50) µs, and (0.6 × 1750) µs] and suggested a new computation method for the calculation of v-t characteristics [60].

Task Force 15.09, led by P. Chowdhuri, compiled a bibliography on the NSLI voltages and reviewed the state of research in 1994 [61]. A comparative study has been done on the behavior of air gaps under transient voltages, generation, and measurements of fast-front impulse voltage waves. In the same year, Chowdhuri et al. experimented the critical BDV levels of different air gaps (rod–rod gap, rod–plane gap and sphere–sphere gap) with various NSLIWS [(0.025 × 0.5) µs, (0.025 × 25) µs, (0.12 × 25) µs, (0.12 × 50) µs, (1.2 × 25) µs, (1.2 × 50) µs, (10 × 50) µs, and (10 × 100) µs] [62]. From the experiment it was observed that the long- and short-time delays for breakdown occurred for fast-front and slow-front impulse waveforms, respectively. Chowdhuri et al. in 1997 performed breakdown tests of rod–rod gap with various NSLI [(1 × 4) µs and {(1.2 ~ 1.4) × (3.2 ~ 3.7)} µs]. One new model was proposed for the calculation of breakdown time. It was revealed that the breakdown

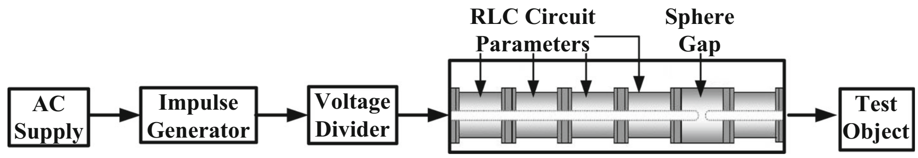

Fig. 9 Schematic diagram of C-2 and E waveform generation [43]

voltage characteristics and the process of breakdown can be replicated by the proposed model [63].

Venkatesan et al. in 2002 had investigated the consecutive strategy for analyzing the impulse toughness of air under NSLI voltage. From the investigation it was observed that the effect on the non-uniform field distribution is sensitive to DE parameters, and an utterly consecutive strategy was established experimentally [6]. X. Q. Zhang experimentally analyzed the characteristics of corona under NSLI in the year 2006 [64]. In [64], a straightforward model was proposed to construct the q-u graph plots for different NSLIW (double exponential and damped oscillatory impulses) through a realistic approach.

In 2007, Ancajima et al. experimented on the reproduction of two medium voltage (MV) insulator's v-t characteristics by applying an SLI (1.2 × 50) µs and a STLI (1.2 × 4) µs [65]. From experimental investigation, it was observed that the longest breakdown time of two MV insulators was 0.3 µs. In [66], Aniserowicz and Zielenkiewicz criticized the non-standard lightning protection devices. From the provided data and theory, it was revealed that the lightning preventers and early streamer emitters were overpriced as well as not so effective as the traditional lightning protection systems. In 2008, K. Bhuyan and S. Chatterjee studied the voltage and current response of power equipment under SLI (1.2 × 50) µs and NSLI (oscillatory waves) [67]. Yuvarajan et al. in [68] measured the breakdown strength of paper composite insulating material under AC, SLI, and NSLI voltage. It was noticed that the dielectric characteristic was compared at room and cryogenic temperature to show the supremacy of the solid insulating materials at liquid nitrogen. In the year 2008, Kadir et al. furnished a few previous research works on the NSLIW and utilized the PSCAD / EMTDC software to reveal the procedure of breakdown. It was observed that the instantaneous voltages were firmly relying on the span of leader and ailing relied on the crest voltage [69].

In 2010, Ancajima et al. presented the results obtained from the experiment performed with STLI [(1.2 × 4) µs] and SLIW [(1.2 × 50) µs] on two types of fiberglass core polytetrafluoroethylene (PTFE) covered insulators and focused on the v-t characteristics [30]. From the experimental results it was confirmed that the v-t characteristics of insulators may be accurately reproduced by Chowdhuri model [63]. In 2010, S. Venkatesan and S. Usa inspected the functioning of NSLI voltage over a short air gap using their newly suggested hyperbolical model [70]. C. P. Braz and A. Piantini in [71] revealed that the critical lightning impulse flashover voltage was always greater for negative polarity with respect to positive polarity after investigating the dielectric response of the distribution insulators for NSLIVs in 2011. In 2012 Braz et al. researched on the forecasting methods by observing the breakdown characteristics of 15 kV porcelain pin type insulators for different types of impulses [(1.2 × 4) µs, (1.2 × 10) µs, and [(1.2 × 50) µs] [72]. From the investigated results it was noticed that the DE Model may be used to forecast the behavior of MV insulators under standard and non-standard impulse voltages.

In the year 2013 Lopes et al. experimented on pin and post type insulators with various types of LIVWs [(0.5 × 5) µs, (0.5 × 10) µs, (0.5 × 20) µs, (0.5 × 50) µs, (1.2 × 5) µs, (1.2 × 10) µs, (1.2 × 20) µs, (1.2 × 50) µs, (3 × 10) µs, (2.9 × 16.1) µs, (4.5 × 16.1) µs, (5 × 20) µs, (5 × 50) µs, and (10 × 50) µs] [73]. From the experiment it was observed that the positive polarity up-down test was good enough to identify the smallest critical flashover voltage. In all trial states for checked insulators, it was noticed that the lightning withstand voltage rises for impulses with fast-front time. In [74], I. A. Metwally has identified that the phase angle sensitivity of Rogowski coil rises with the rise in the coil ending resistance, followed by deformation of the impulse waveform.

K. Bhuyan and S. Chatterjee in 2015 investigated the response of SLI and NSLIVWs on surge arresters [75]. From the results, it was found that NSLIs can develop higher voltage stress and cause a significant threat to the surge arresters. In 2015, G. Krithika and S. Usa have experimented with air insulation by utilizing the suggested advanced DE model [76]. A few types of LIVs [(1.2 × 50) µs, (1.2 × 44) µs, (1.2 × 55) µs, (0.8 × 50) µs, steep fronted overvoltage (0.58 × 50) µs and very fast transient overvoltage (VFTO) (0.09 × 50) µs] have been applied during the experiment. From the experimental results it was observed that the suggested DE model precisely forecasted the v-t characteristics of different insulation for various impulse overvoltages. In 2016, M. Shigihara and A. Piantini analyzed the critical flashover overvoltage [77]. The v-t characteristics curve of a standard 24 kV porcelain pin-type insulator was obtained for five LIVWs (1.2 × 4 µs, 1.2 × 10 µs, 1.2 × 50 µs, 3 × 10 µs, and 7.5 × 30 µs), of both polarities. Bhattacharyya et al., in 2016, through their investigation on the electric stress on an MV cable termination, showed that the highest electric stress due to different applied impulse voltage waveforms was detected at the earthed screen and the implanted diverter interface. It was found that the electric stress was higher for standard and non-standard chopped impulse waveforms. For all the impulse voltage waveforms, expanding the deflector angle could make the more uniform potential distribution at the interface [78]. In the year 2016, Huang and Zhang constructed an experimental system for the computation and comparison of the corona charge–voltage (q-u) curves under NSLIW (damped oscillation and double exponential impulses) [79]. Lopes et al. in [80] examined the critical flashover voltages and v-t characteristics curve for a few different LIVWs [(0.5 × 5) μs, (0.5 × 20) μs, (1.2 × 10) μs, (1.2 × 50) μs, (3 × 16) μs, (5 × 50) μs]. It was found that the negative polarity impulse is riskier for cut-out fuses (15–25) kV.

In 2018, Shigihara et al. modified a Marx impulse generator by varying the circuit parameters to generate the four selected NSLIWs [(1.2 × 4) μs, (1.2 × 10) μs, (3 × 10) μs, and (7.5 × 30) μs] and the SLI (1.2 × 50) μs [81]. The crucial dissimilarities were observed after comparing the four NSLIs with respect to SLI. In 2019, Jana et al. analyzed the numerical computation of non-standard lightning impulse energy storage system using impulse generator [1]. It was found that a single-stage two-level spark generator circuit with multi-level inverter integrated with supercapacitor was designed to simulate real-time non-standard lightning energy storing system. Mahmood et al. in 2019 utilized a risk-based insulation coordination technique to analyze the application of various lightning protection schemes of medium-voltage overhead lines [82]. Faria et al. in 2020 attempted to compare the withstand tests of MV switches and cut-out fuses with six LIVWs of both polarities [(0.5 × 5) μs, (0.5 × 20) μs, (1.2 × 10) μs, (1.2 × 50) μs, (3 × 16) μs, and (5 × 50) μs] [10]. From the results it was obtained that the negative polarity impulses are more harmful with respect to positive polarity. In [83], Liang et al. proposed a new non-intrusive technique to evaluate transient electric field distribution. It was observed that in time domain, the measured and calculated electric fields are absolutely same for impulse voltages. In 2021, H. M. Wickert and T. B. Marchesan suggested a new multiresolution wavelet analysis-based technique to simulate NSLIW for impulse tests in laboratories [84]. Various changes (magnitude, rise-time, and cut-off instant) were suggested on standard lightning impulse test to generate NSLIW. In 2022 Jana et al. proposed an impulse island controller to extricate and control the high voltage non-standard lightning impulse for storing in a supercapacitor [2].

The literature on the effect of non-standard lightning over the insulation of high voltage equipment is discussed in the next section.

6 The effect of non-standard lightning surge voltage waveform over the insulation of high voltage equipment

According to literature survey, it was found that several researches have been performed on the effect of non-standard lightning impulse (NSLI) on the insulation of HV equipment. A brief overview of the research outcome has been presented below.

In 1973, Caldwell and Darveniza experimentally and analytically attempted to forecast the behavior of insulation when stressed by NSLIWs [85]. From the results it was observed that for positive polarity, the deviation between the experimental and analytical data was lesser with respect to negative polarity. T. Suzuki and K. Miyake in 1977 identified that the streamers and leaders have the major influences on the time of breakdown [86]. The experiments were performed with two NSLIVWs [(3 × 12) μs and (2.5 × 53) μs] over rod–plane gaps [(1–5 m) and (2 m & 3 m)] and rod–rod gaps [(2–5 m)]. In 1998, Koto et al. compared nine NSLIWs [{Waveform-A: A_1: (0.20 × 0.26) μs; A_2: (0.28 × 0.29) μs; A_3: (0.60 × 1.15) μs}, {Waveform-B: B_1: [(0.26 × 0.71) μs; E_2/E_1: 0.82]; B_2: [(0.76 × 1.34) μs; E_2 / E_1: 0.73]; B_3: [(0.98 × 5.00) μs; E_2/E_1: 0.88]} and {Waveform-C: C_1: [(0.20 × 0.28) μs; E_2/E_1: 0.80; E_3/E_1: 0.66], C_2: [(0.32 × 0.28) μs; E_2/E_1: 0.90; E_3/E_1: 0.82]; C_3: [(0.52 × 0.57) μs; E_2/E_1: 0.82; E_3/E_1: 0.68]}] with SLIW (1.2 × 50 μs). From the research it was found that the flashover voltage of shorter wavefront was higher with respect to the minimum flashover voltage of SLIW [40].

Okabe et al. in [87] inspected about the dielectric characteristics (oil gaps and insulation between turns and models of insulation between sections) of oil-filled transformers under NSLIVs. It was observed that the BDV under oscillatory impulse voltages was higher in comparison with the SLIVs in the frequency span of (400 kHz–1 MHz). In [41], the authors have analyzed the insulation properties in SF_6 gas with SLI [(1.2 × 50) μs] and a few NSLIWs [{Waveform-A: A_1: (0.60 × 1.15) μs; A_2: (0.85 × 1.65) μs; A_3: (0.28 × 0.29) μs; A_4: (0.20 × 0.26) μs}, {Waveform-B: B_1: [(0.76 × 1.34) μs; E_2/E_1: 0.73]; B_2: [(0.84 × 2.56) μs; E_2/E_1: 0.81]; B_3: [(0.98 × 5.00) μs; E_2/E_1: 0.88]; B_4: [(0.26 × 0.71) μs; E_2/E_1: 0.82]} and {Waveform-C: C_1: [(0.32 × 0.28) μs; E_3/E_1: 0.90; (1.7 MHz)]; C_2: [(0.52 × 0.57) μs; E_3/E_1: 0.82; (0.9 MHz)]; C_3: [(1.2 × 1.40) μs; E_3/E_1: 0.75; (0.4 MHz)]; C_4: [(0.20 × 0.28) μs; E_3/E_1: 0.82; (2.3 MHz)]}]. From the results it was found that the insulation does not face serious issues while encountering the shorter fronted impulse waveform. In [88], the authors have showed that mean BDV of turn-to-turn model is 1.5 times higher for NSLIVW with respect to SLIVW. Then the authors inspected on the generation of single-frequency and double-frequency oscillatory waveforms and the attributes of insulation under NSLIWs

[49]. From the test results it was recognized that insulation properties (V_{min}) were (15–24) % and (6–13) % higher for single-frequency oscillatory and double-frequency oscillatory waveforms, respectively, with respect to SLIW.

Usa et al. had shown to have sustainable success for unidirectional oscillating voltages while measuring the insulation strength for NSLWs using the modified DE method in 2002 [89]. In [90], Rokunohe et al. have inspected the properties of SF_6 gas breakdown by changing the polarity of five pulse-type (A-waveform) NSLIWs [A_1: (0.20 × 0.26) µs; A_2-1: [(0.28 × 0.29)] µs; A_2-2: [(0.27 × 0.28)] µs; A2-3: [(0.23 × 0.22)] µs; A_3: (0.6 × 2.0) µs]. It was observed that the minimum breakdown voltage (BDV) (V_{min}) is 10% more for NSLIWs with respect to SLI (LV_{min}). S. Okabe and S. Yuasa had investigated the evaluation method for NSLIW (A–D) of (oil gap, insulation between turns, and insulation between sections) oil-filled transformer in the year 2003. It was found that NSLIWs may be converted to SLIW, and crest value was reduced [91]. In [42], the authors have developed an experimental circuit to generate NSLIWs (A-D) and achieved almost similar waveforms as obtained by using EMTP. It was noticed that the breakdown voltage for gas insulated switchgear in NSLIW was (15–25) % higher than SLIW. In the same year, same group of authors inspected about properties of SF_6 gas breakdown by applying eight NSLIWs [waveform-A: (For Gas Gap): A_1: (0.20 × 0.26) µs, A_2: [(0.28–0.28) × (0.22–0.29)] µs, A_3: (0.32 × 0.58) µs, A_4: (0.60 × 1.15) µs, A_5: (0.85 × 1.65) µs; (For Spacer): A_6: (0.30 × 0.34) µs, A_7: (0.60 × 1.50) µs, A_8: (0.91 × 1.84) µs]. It was observed that the experimental V_{min} for SF_6 gas under NSLIWs is more than LV_{min} of SLI [92].

In 2004, Sathish et al. experimented with [(1.2 × 50) µs, (1.6 × 80) µs and (1.2 × 23) µs] impulses to estimate the v-t characteristics of various thicknesses OIP insulation [93]. It was found that the regression analysis was utilized to establish the developed mathematical model. Okabe et al. in [94] investigated the dielectric characteristics of (oil gap, insulation between turns, and insulation between sections) oil-filled transformers in the presence of NSLIWs. From the results it was revealed that the B-type waveform's breakdown occurs in sharp wavefront section rather than wave tail region. In the year 2004, S. Okabe and S. Yuasa investigated the evaluation method of NSLIWs for SF_6 gas and spacer insulation and showed that NSLIWs are converted into equivalent SLIWs. It was observed that due to significant attenuation, NSLIW is less harmful for insulation [95].

S. Venkatesan and S. USA, in 2005, experimentally found v–t characteristics for various gap distances using SLIW [(1.2 × 50) µs] by using the DE model [96]. It was found that the percentage error between the actual time of breakdown and estimated time is less than 10%. In the year 2005, Ancajima et al. experimented on the breakdown features of MV insulators by using STLI [(1.2 × 4) µs] and SLI [(1.2 × 50) µs] [97]. From the experiments, it was observed that the model suggested by Chowdhuri et al. [63] was superior in forecasting for LIs irrespective of their polarity, and the 50% BDV of SLI was (7–27) % less than STLI because of the higher insulation pressure of STLI.

In 2006, Yokoi et al. investigated the insulation attributes of CO_2 gas for single-frequency oscillatory waveforms with several frequencies from 5.3 to 20 MHz and damping ratios [50]. From the investigation it was revealed that in the case of $\tau_d = 0.15$ µs to 5.1 µs, the NSLIW's V_{min} were (8–36) % more than SLI's V_{min} in CO_2. Kaneko et al. in the same year inspected the process of assessment for actual LI based on insulation features for the CO_2 gas gap [98]. In [51], the authors have explained the insulation features of CO_2 gas for single-frequency oscillatory waveforms with different frequencies (1.3 to 4.0 MHz). From the investigation it was observed that no significant changes were found in the v-t characteristics curve while changing the damping of the oscillation.

S. Venkatesan and S. USA in [99] have examined the impulse strength of transformer insulation with NSLIWs. From the investigation it was recognized that the functioning of insulation under unidirectional NSLIWs has been estimated with the help of v–t characteristics and the DE method. S. Okabe in [100] showed that for NSLIW (A and B-waveform), mean BDV of oil-immersed transformers were greater with respect to mean BDV under the SLIW. The authors in [101] showed that for NSLIW (C and D-waveform), the mean BDV of oil-immersed transformers were lesser for SLIW with respect to damped-oscillation waveform and rising oscillation waveform, respectively. In [52], S. Kaneko and S. Okabe have examined insulation characteristics of N_2 gas for a non-standard lightning impulse waveform having different frequencies (2.7 MHz–20.0 MHz) and damping ratios. From the experiment it was found that the with respect to numerous frequencies, the lowest V_{min} recognized were (9–20)% more than V_{min} of SLI in N_2 [52].

In 2008, S. Okabe and J. Takami examined an evaluation method of the oil-immersed transformer (oil gaps, insulation between turns, and insulation between sections) for NSLIWs [11]. It was observed that NSLIWs were usually less dangerous for winding insulation with respect to SLIWs. In [53], Okabe et al. obtained the dielectric breakdown v-t characteristics of the SF_6 gas gap for various conditions. It was recognized that the dielectric breakdown voltage was (6–36)% higher for NSLIW with respect to SLI. For C-2 waveform, V_{min} increased with the decrease of damping time constant (τ_d) while the frequency is kept constant. For E-waveform, V_{min} remained same irrespective of frequencies when damping time constant (τ_d) is kept constant.

In [102], an attempt has been made by Mitra et al. to recognize the voltage stress on transformer winding insulation under various types of terminal excitation. They have optimized the design of insulation of HV transformer and established that severe stress on insulation occurs if terminal excitation frequency matches with any of winding's inherent frequencies. As a result, it may lead to damage of transformer and transformer winding insulation [102]. In [103], Okabe et al. analyzed the K-factor technique by applying the insulation properties under an overshoot waveform in NSLIW.

K. Bhuyan and S. Chatterjee in [12] have simulated standard and NSLIW on power transformer. It was observed that the major and minor level impact occur on power transformer insulation due to SLIW and NSLIW, respectively. The high voltage stress was developed in between the winding and ground of transformer by SLIW due to its long-tail time. The higher voltage stress was observed at the middle of the winding due to chopped impulses. In [54], Wada et al. experimentally investigated the insulation attributes of N_2 gas for NSLIs [Double (E-waveform) and Single (C2-waveforms] frequency oscillation waveforms) and assembled information for better designing of insulation. It was noticed that for the quasi-uniform electric fields, very severe damage may be caused by negative polarity of both the waveforms.

In [104] Wang et al. showed that the insulation between turns model could tolerate the excess oscillating NSLIWs with respect to SLIWs by investigating the breakdown properties of sphere-plate system and between turns insulation model. By using the hyperbolic model, G. Krithika and S. USA mathematically modeled the v-t characteristics in the same year [105]. The investigation recognized that the effect of oscillatory waves was more with respect to their equivalent lightning impulses, and the breakdown strength of oil impregnated paper (OIP) was inversely proportional to the frequency of oscillation [105]. Sankarganesh et al. in [106] tried to construct a technique to investigate the observation of the breakdown characteristics of a transformer winding insulation under NSLIV. From the results it was revealed that the BDV of transformer winding insulation was higher with respect to standard lightning impulse voltages (SLIVs) under oscillatory impulse voltages (400 kHz–1 MHz). Sarathi et al. showed that BDV of liquid N_2 is higher for the negative polarity of unidirectional oscillatory impulse voltage (UOIV) (25 kHz–65 kHz) and oscillatory impulse voltages (OIVs) [107].

K. Bhuyan and S. Chatterjee in [13] investigated the electric stresses on transformer winding insulation for SLI and NSLIVs (0.8×2.8) μs. It was found that NSLIVWs build up HV stresses, which produces the highest threat to equipment's insulation. The peak value, steepness, and front and tail of impulse wave had an essential role in finding out the insulation's functioning [13]. In [108], the v–n characteristic of OIP insulation under impulse voltage with different waveforms was experimentally achieved by Sun et al. From the experimental results, it was observed that the OIP insulation displays superior insulating performance to resist continuous NSLIVW. The BDV of OIP insulation is depended on the wavefront time of the applied impulse waveform.

In [109], Wang et al. suggested that the BDV of paper insulation increased with the reduction in front time. In [110], Wang et al. researched on the breakdown characteristics for oil-paper insulation under LIWs with oscillations. From the experimental results it was revealed that the rise in BDV is inversely proportional to wavefront time. Oil-paper insulation could resist higher low frequency-oscillating LIWs with respect to SLIW [110]. In [111], Hua et al. inspected the v–n characteristics of polypropylene (PP) film and oil-impregnated paper (OIP) with various waveforms [(0.24×50) μs, (0.4×50) μs, (0.72×50) μs, (1.2×50) μs, (3.3×50) μs, (6×50) μs, (1.2×25) μs, (1.2×100) μs, (1.2×198) μs, and (1.2×500) μs], respectively. From the experimental study, it was found that the impulse voltage surviving capability of OIP PP film is proportional and inversely proportional to the time of the wavefront and time to wave tail, respectively. In [112] Zhou et al. analyzed the regulation of rise-time and overshoot of impulse voltage waveform for transformer having large entrance capacitance through simulation as well as experiments. The rise-time of the impulse waveform has been varied in the range of (2.04–2.16 μs). From the result, it was observed that the surge protective device performed much better while connected to the twisted line rather than attached with parallel or ring line [112].

In [113], Z. A. Mubarak and S. Usa experimentally demonstrated that the dielectric breakdown strength of OIP decreases under different waveshapes [17% for SLI, 2% for VFTO] as the paper insulation thickness rises from 0.25 to 0.75 mm. In [114], Florkowski et al. have compared the response of transformer winding under different impulse voltages. From the research work it was observed that the transformer generally has few resonant frequencies. The maximum value of overvoltage inside the transformer winding will be reached if the frequency of the oscillating NSLIW matches with the resonant frequency of transformer.

7 Conclusion and future scope

This paper involves a detailed and comprehensive study regarding the non-standard lightning impulse waveforms published over the last century. From the literature survey, it can be observed that the classified parameters of NSLIW are somehow different from standard lightning impulse. From this study, identification of non-standard lightning impulse voltage and the effects of different non-standard lightning impulse voltage waveforms on the high voltage equipment can be recognized. Therefore, this study will be beneficial for the researchers to get relevant information about the

NSLIW. Further, with this information, the design of the electrical insulation may be modified to withstand the NSLIW. Moreover, the life expectancy of power equipment will be enhanced.

As a future scope, an experimental circuit for generating non-standard lightning impulse waveforms will be verified in laboratory. The generated non-standard lightning impulse waveforms will be applied to different types of insulation (like OIP, XLPE, silicon rubber insulator, etc.) to study the effect of NSLIW on electrical insulation.

References

1. Jana S, Biswas P K, Das U (2018) Numerical computational analysis of lightning energy storage system using single stage two level impulse generator. In: 2nd international conference on power, energy and environment: towards smart technology (ICEPE) (2018): 1–6
2. Jana S, Biswas PK, Sain C (2022) Mathematical modeling of impulse Island controller to safely store the energy from high voltage lightning impulse. Energy Storage 2022:1–11. https://doi.org/10.1002/est2.325
3. High Voltage Test Techniques Part 1: General Definitions and Test Requirements, Standard IS 2071–1, Indian Standard (2004)
4. High-voltage Test Techniques-Part 1: General Definitions and Test Requirements, Standard IEC 60060–1, International Electrotechnical Commission (2010)
5. High-Voltage Test Techniques: IEC Publication 60 (1962)
6. Venkatesan S, Usa S, Kumar KU (2002) Unconditionally sequential approach to calculate the impulse voltages strength of air for non-standard impulse voltages. In: Proceedings IEEE/PES Asia Pacific transmission and distribution conference and exhibition. 2: 1236–1240
7. Okabe S, Yuasa S, Kaneko S (2007) Evaluation of breakdown characteristics of gas-insulated switchgear for non-standard lightning impulse waveforms -analysis and generation circuit of non-standard lightning impulse waveforms in actual field. IEEE Trans Dielectr Electr Insul 14(2):312–320
8. Ueta G, Wada J, Okabe S (2011) Evaluation of breakdown characteristics of CO_2 gas for non-standard lightning impulse waveforms - method for converting non-standard lightning impulse waveforms into standard lightning impulse waveforms-. IEEE Trans Dielectr Electr Insul 18(5):1724–1733
9. Wada J, Ueta G, Okabe S (2013) Evaluation of breakdown characteristics of N_2 gas for non-standard lightning impulse waveforms - method for converting non-standard lightning impulse waveforms into standard lightning impulse waveforms-. IEEE Trans Dielectr Electr Insul 20(2):505–514
10. Faria GH et al (2020) Lightning withstand of medium voltage switches and cut-out fuses considering standard and non-standard impulse shapes. IEEE Electr Insul Mag 36(4):47–55
11. Okabe S, Takami J (2008) Evaluation of breakdown characteristics of oil-immersed transformers under non-standard lightning impulse waveforms - method for converting non-standard lightning impulse waveforms into standard lightning impulse waveforms. IEEE Trans Dielectr Electr Insul 15(5):1288–1296
12. Bhuyan K, Chatterjee S (2010) Study of effects of standard and non-standard impulse waves on power transformer. In: Proc Power Electr Drives and Energy Syst Int Conf (2010): 1–4
13. Bhuyan K, Chatterjee S (2015) Electric stresses on transformer winding insulation under standard and non-standard impulse voltages. Electric Power Sys Res 123:40–47
14. AIEE Committee Report (1934) Flashover voltages of insulators and gaps. Elect Eng 53(6):882–886
15. Carrus A, Funes LE (1984) Very short-tailed lightning double exponential wave generation techniques based on Marx circuit standard configurations. IEEE Trans. Power App Syst PAS-103(4):782–787
16. Burrage LM, Veverka EF, McConnell BW (1987) Steep front short duration low voltage impulse performance of distribution transformers. IEEE Trans Power Del PWRD 2(4):1152–1156
17. Carrus A (1989) An inductance on the Marx generator tail branch. New technique for high efficiency laboratory reproduction of short time to Half value lightning impulses. IEEE Trans Power Del 4(1):90–94
18. Lux E, Miller DB, Kempkes DL (1989) The effect of steep-front short-duration pulses on polyethylene cable insulation. In: Proc IEEE Eng Info Tech in the Southeast 1989. vol 3, pp 1372–1376
19. Shaw JH (1989) Instrumentation system used to determine the effects of steep front short duration impulses on electric power system Insulation. IEEE Trans Power Del 4(2):938–941
20. Aoshima Y, Miyake K (1989) Flashover characteristics of air gaps for short tail waves (Japanese). The Trans Ins Elect Eng Japan B 109(3):135–142
21. Miller DB, Lux AE, Barnes PR (1990) The effects of steep-front, short-duration impulses on power distribution components. IEEE Trans Power Del 5(2):708–714
22. Grzybowski S, Jacob PB (1990) The steep-front, short-duration pulse characteristics of distribution insulators with wood. IEEE Trans Power Del 5(3):1608–1616
23. Motoyama H (1996) Experimental study and analysis of breakdown characteristics of long air gaps with short tail lightning impulse. IEEE Trans Power Del 11(2):972–979
24. Carrus A et al (1999) Short tail lightning impulse behaviour of medium voltage line insulation. IEEE Trans Power Del 14(1):218–226
25. Venkatesan S, Ranjan PV, Ashokaraju D (2003) A comparative study on methods for evaluation of lightning impulse parameters. In: Proc Asia-Pacific Region Convergent Tech Conf (TENCON 2003), 2003. vol 4, pp 1562–1566
26. Grzybowski S, Song Y, Kappenman J (2004) CFO voltage and V-t characteristic of 15 kV polymer suspension insulator under lightning and Steep front short duration impulses. In: Proc IEEE Int Symp Elect Insul Conf. pp 308–311
27. Grzybowski S, Song S, Kappenman J (2004) Study on the electrical strength of distribution insulators under steep front, short-duration pulse. In: Proc Electr Insul Dielectr Phenomena Conf 2004. pp 643–646
28. Ancajima A et al (2007) Breakdown characteristics of air spark-gaps stressed by standard and short-tail lightning impulses: experimental results and comparison with time to sparkover models. J Electrostatics 65(5–6):282–288
29. Braz CP et al (2014) Analysis of different procedures for the application of the disruptive effect model to distribution insulators Subject to short tail lightning impulses. Electr Power Syst Res 113:165–170
30. Ancajima A et al (2010) Behavior of MV insulators under lightning-induced overvoltages: experimental results and reproduction of volt-time characteristics by disruptive effect models. IEEE Trans Power Del 25(1):221–230
31. Lantharthong T et al (2014) Effect of waveform and impulse resistance on lightning performance in distribution system. In: Proc IEEE Int Conf Lightning Protection (ICLP). pp 1766–1769

32. Wang X, Yu Z, He J (2014) Breakdown process experiments of 110- to 500-kV insulator strings under short tail lightning impulse. IEEE Trans Power Del 29(5):2394–2401
33. Yuan Z et al (2014) Experimental study and analysis of insulator breakdown characteristics with short-tail lightning impulse. J Int Council on Elect Eng 4(3):199–203
34. Sima W et al (2016) Impact of time parameters of lightning impulse on the breakdown characteristics of oil-paper insulation. High Volt 1(1):18–24
35. Yamamoto K, Masuda K, Sumi S (2018) Long-wave-tail current Generator to generate real winter lightning current. In: Proceedings of 34th international conference on lightning protection (ICLP). pp 1–5
36. Xiao P et al (2018) Experimental study on the flashover characteristics of polluted insulators under short-tail lightning impulse waveform. In: Proc IEEE Int Conf High Volt Eng App (ICHVE). pp 1–4
37. Zhao X et al (2018) Breakdown characteristics of a 220-kV composite insulator string under short tail lightning impulses based on the discharge current and images. IEEE Trans Power Del 33(6):3211–3217
38. Han Y et al (2018) Study on influencing factors of insulators flashover characteristics on the 110 kV true tower under the lightning impulse. IEEE Access 6:66536–66544
39. Okabe S et al (2009) Evaluation of breakdown characteristics of gas-insulated switchgear for non-standard lightning impulse waveforms -method for converting non-standard lightning impulse waveforms into standard lightning impulse waveforms-. IEEE Trans Dielectr Electr Insul 16(1):42–51
40. Koto M et al (1998) Insulation characteristics of GIS for non-standard lightning surge waveforms. In: Proc 8th Int Sym Gaseous Dielectr (1998). pp 547–553
41. Okabe S et al (1999) Insulation characteristics of GIS for non-standard lightning surge waveforms < No-2: gas gaps and spacer surface >. In: Proc Eng Symp High Volt (1999). vol 3, pp 163–166
42. Okabe S et al (2003) Analysis of non-standard lightning impulse voltage for actual substation and generation circuit (Japanese). IEEJ Trans Power Energy 123(2):175–180
43. Wada J, Ueta G, Okabe S (2012) Evaluation of breakdown characteristics of CO_2 gas for non-standard lightning impulse WAVEFORMS - breakdown characteristics under double-frequency oscillation waveforms and single-frequency oscillation waveforms in the presence of bias voltage. IEEE Trans Dielectr Electr Insul 19(5):1799–1809
44. Ueta G, Wada J, Okabe S (2011) Evaluation of breakdown characteristics of CO2 gas for non-standard lightning impulse waveforms - breakdown characteristics under single-frequency oscillation waveforms of 5.3 MHz to 20.0 MHz. IEEE Trans Dielectr Electr Insul 18(1):238–245
45. Wada J, Ueta G, Okabe S (2011) Evaluation of breakdown characteristics of CO_2 gas for non-standard lightning impulse waveforms under non-uniform electric field - breakdown characteristics for Single-frequency oscillation waveforms. IEEE Trans Dielectr Electr Insul 18(2):640–648
46. Wada J, Ueta G, Okabe S (2011) Evaluation of breakdown characteristics of N_2 gas for non-standard lightning impulse waveforms - breakdown characteristics under single-frequency oscillation waveforms and with bias voltages. IEEE Trans Dielectr Electr Insul 18(5):1759–1766
47. Wada J, Ueta G, Okabe S (2013) Evaluation of breakdown characteristics of CO_2 gas for non-standard lightning impulse waveforms - breakdown characteristics in the presence of bias voltages under non-uniform electric field. IEEE Trans Dielectr Electr Insul 20(1):112–121
48. Wada J et al (2014) Evaluation of breakdown characteristics of CO_2 gas for non-standard lightning impulse waveforms - breakdown characteristics for double-frequency oscillation waveforms under non-uniform electric field. IEEE Trans Dielectr Electr Insul 21(2):617–626
49. Okabe S et al (2001) Insulation characteristics of GIS under non-standard lightning impulse oscillations - insulation characteristics under high frequency oscillations- (Japanese). T IEE Japan 121-B(11):1587–1593
50. Yokoi T, Kaneko S, Okabe S (2006) Insulation characteristics of CO2 gas for non-standard lightning impulse oscillations - insulation characteristics under single-frequency oscillations from 5.3 to 20 MHz- (Japanese). T IEE Japan 126(5):539–544
51. Kaneko S, Yokoi T, Okabe S (2006) Insulation characteristics of CO2 gas for non-standard lightning impulse oscillations - insulation characteristics under single-frequency oscillations from 1.3 to 4.0 MHz- (Japanese). IEEJ Trans PE 126(1):91–96
52. Kaneko S, Okabe S (2007) Insulation characteristics and its evaluation of N_2 gas for non-standard lightning impulse waveforms (Japanese). IEEJ Trans PE 127(7):854–862
53. Okabe S, Yuasa S, Kaneko S (2008) Evaluation of breakdown characteristics of gas-insulated switchgear for non-standard lightning impulse waveforms - breakdown characteristics for non-standard lightning impulse waveforms associated with disconnector switching surges-. IEEE Trans Dielectr Electr Insul 15(3):721–729
54. Wada J, Ueta G, Okabe S (2013) Evaluation of breakdown characteristics of N_2 gas for non-standard lightning impulse waveforms - breakdown characteristics under double-frequency oscillation waveforms and pressure-distance characteristics. IEEE Trans Dielectr Electr Insul 19(5):1810–1818
55. Jones AR (1954) Evaluation of the integration method for analysis of non-standard surge voltages. AIEE Trans 73:984–990
56. Shindo T, Suzuki T (1985) A new calculation method of breakdown voltage-time characteristics of long air gaps. IEEE Trans Power App Syst PAS- 104(6):1556–1563
57. Li Z, Kuffel R, Kuffel E (1986) Volt-time characteristics in air, SF_6/AIR mixture and N_2 for coaxial cylinder and rod-sphere gaps. IEEE Trans Elect Insul EI- 21(2):151–155
58. Darveniza M, Vlastos AE (1988) Generalised breakdown models and the integration method for predicting non-standard waveshape impulse strengths. In: Proc of Prop and Appl of Dielectr Mater Sec Int Conf (1988). vol 1, pp 284–287
59. Darveniza M, Vlastos AE (1988) The generalized integration method for predicting impulse volt-time characteristics for non-standard wave shapes - a theoretical basis. IEEE Trans Electr Insul 23(3):373–381
60. Pigini A et al (1989) Performance of large air gaps under lightning overvoltages: experimental study and analysis of accuracy predetermination methods. IEEE Trans Power Del 4(2):1379–1392
61. Task Force 15.09 on Non-standard Lightning Voltage Waves, Lightning and Insulator Subcommittee of the T & D Committee (1994) Review of research on non-standard lightning voltage waves. IEEE Trans Power Del 9(4):1972–1981
62. Chowdhuri P et al (1994) The effects of non-standard lightning voltage waveshapes on the impulse strength of short air gaps. IEEE Trans Power Del 9(4):1991–1999
63. Chowdhuri P, Mishra AK, McConnell BW (1997) Volt-time characteristics of short air gaps under non-standard lightning voltage waves. IEEE Trans Power Del 12(1):470–476
64. Zhang XQ (2006) Study on corona characteristics under non-standard lightning impulses. Electr Eng 89:519–524
65. Ancajima A et al (2007) Optimal selection of disruptive effect models parameters for the reproduction of mv insulators volt-time characteristics under standard and non-standard lightning impulses. IEEE Lausanne Power Tech 760–765

66. Aniserowicz K, Zielenkiewicz M (2007) Non-standard Lightning Protection Devices-A Criticism. In: Proc Int Conf Electr Contr Tech: 177–180.
67. Bhuyan K, Chatterjee S (2008) Study of effect of standard and non-standard impulse waves on power equipments. In: Proc NCEEERE (2008). pp 1–6
68. Yuvarajan M et al (2008) Behavior of LN_2/ Paper composite insulating material under AC, standard and non-standard lightning impulse voltage. In: Proc Electr Insul Dielectr Phenomena Conf (2008). pp 641–644
69. Kadir MZAA, Ahmad MH, Jasni J (2008) Effect of the non-standard lightning current and waveshape on lightning surge analysis. Asian J Appl Sci 1(2):168–176
70. Venkatesan S, Usa S (2010) Volt–time characteristics of small airgaps with hyperbolic model. Electr Power Syst Res 80(7):739–742
71. Braz P, Piantini A (2011) Analysis of the dielectric behavior of distribution insulators under non-standard lightning impulses voltages (Portuguese). IEEE Lat Am Trans 9(5):732–739
72. Braz P et al (2012) Analysis of the disruptive effect model for the prediction of the breakdown characteristics of distribution insulators under non-standard lightning impulses. In: Proc Lightning Protection Int Conf (2012). pp 1–7
73. Lopes G P, Pedroso J A D, Martinez M L B (2013) Evaluation of CFO for medium voltage insulators submitted to non-standard impulse shapes experimental results. In: Proc IEEE Electr Insul Conf (EIC) (2013). pp 419–423
74. Metwally IA (2013) Performance improvement of slow-wave rogowski coils for high impulse current measurement. IEEE Sens J 13(2):538–547
75. Bhuyan K, Chatterjee S (2015) Simulation of overvoltage stresses on surge arrester insulation. Int Trans Electr Energy Syst 26(6):1210–1225
76. Krithika G, Usa S (2015) v-t Characteristics using extended disruptive effect model for impulses of varying front times. IEEE Trans Dielectr Electr Insul 22(4):2191–2195
77. Shigihara M, Piantini A (2016) Volt-time curves of 24 kV porcelain insulators under non-standard impulse waveshapes. In: Proc Lightning Protection (ICLP) Int Conf (2016). pp 1–5
78. Bhattacharyya S et al (2016) Electric stress analysis of a medium voltage cable termination subjected to standard and non-standard lightning impulse voltages. In: Proc Intelligent Contr Power Instru (ICICPI) Int Conf (2016). pp 169–173
79. Huang K, Zhang X (2016) An experimental study on corona q-u curves under non-standard lightning impulses. J Electrostatics 81:37–41
80. Lopes G P et al (2016) Lightning withstand of medium voltage cut-out fuses stressed by non-standard impulse shapes experimental results. In: Proc IEEE Electr Insul Conf (EIC) (2016). pp 210–214
81. Shigihara M et al (2018) Generation of non-standard lightning impulse unipolar waveshapes. In: Proc IEEE High Volt Eng App (ICHVE) Int Conf (2018). pp 1–4
82. Mahmood F, Rizk MdEM, Lehtonen M (2019) Risk-based insulation coordination studies for protection of medium-voltage overhead lines against lightning-induced overvoltages. Electr Eng (Springer) 101:311–320
83. Liang H, Du B, Li J (2020) Non-intrusive measurement of transient electric field distribution under AC and impulse voltages. IEEE Sens J 20(18):10898–10902
84. Wickert HM, Marchesan TB (2021) A method for representing non-standard waveform in factory tests using impulse waveforms. IEEE Trans Power Del 1–10, 2021 [Online]. Available: https://doi.org/10.1109/TPWRD.2021.3129603
85. Caldwell RO, Darveniza M (1973) Experimental and analytical studies of the effect of non-standard waveshapes on the impulse strength of external insulation. IEEE Trans Power App Syst PAS 92(4):1420–1428
86. Suzuki T, Miyake K (1977) Experimental study of breakdown voltage-time characteristics of large air gaps with lightning impulses. IEEE Trans Power App Syst 96(1):227–233
87. Okabe S et al (1999) Dielectric characteristics of oil-filled transformer insulation models under non-standard lightning impulse voltages. In: Proc Eng Symp High Volt (1999). (467): 345–348
88. Okabe S et al (2001) Dielectric characteristics of oil-filled transformer under non-standard lightning surge waveforms: dielectric characteristics of oil-filled transformer insulation models under fast Front short-duration impulse voltages (Japanese). IEEJ Trans Power Energy 121(6):775–781
89. Savadamuthu U, Udayakumar K, Jayashankar V (2002) Modified disruptive effect method as a measure of insulation strength for non-standard lightning waveforms. IEEE Trans Power Del 17(2):510–515
90. Rokunohe T et al (2002) Insulation characteristics of SF_6 gas for non-standard impulse voltages polarity reversal pulse waveforms (Japanese). T IEE Japan 122-B(11):1232–1237
91. Okabe S, Yuasa S (2003) Evaluation method of non-standard lightning impulse waveform for oil-filled transformer. IEEJ Trans Power Energy 123(12):1580–1586
92. Yuasa S, Okabe S (2003) Breakdown characteristics of SF_6 gas for non-standard lightning impulse voltage - insulation characteristics of gas gap and spacer surface under single pulse waveform- (Japanese). IEEJ Trans PE 123(10):1242–1249
93. Kumar JSS et al (2004) Effective model for prediction of impulse strength of oil-impregnated paper insulation under non-standard impulse voltages. In: Proc Power Syst Tech Int Conf (POWERCON) (2004). pp 1619–1622
94. Okabe S et al (2004) Dielectric characteristics of oil-filled transformer in the presence of non-standard lightning surge waveforms. Electr Eng Jpn 146(3):39–45
95. Okabe S, Yuasa S (2004) Evaluation method of non-standard lightning impulse waveforms for GIS (Japanese). IEEJ Trans PE 124(1):156–161
96. Venkatesan S, Usa S (2005) Impulse volt-time characteristics of oil and OIP insulation. Am J App Sci 2(2):591–596
97. Ancajima A et al (2005) Breakdown characteristics of MV distribution and electric traction lines insulators stressed by standard and short tail lightning impulses. In: 2005 IEEE Russia Power Tech. pp 1–7
98. Kaneko S, Yokoi T, Okabe S (2006) Insulation characteristics of CO_2 gas for non-standard lightning impulse oscillations - evaluation method of non-standard lightning impulse waveform for CO_2 gas insulation- (Japanese). IEEJ Trans PE 126(7):701–707
99. Venkatesan S, Usa S (2007) Impulse strength of transformer insulation with non-standard waveshapes. IEEE Trans Power Del 22(4):s4-2221
100. Okabe S (2007) Evaluation of breakdown characteristics of oil-immersed transformers under non-standard lightning impulse waveforms - definition of non-standard lightning impulse waveforms and insulation characteristics for waveforms including pulses-. IEEE Trans Dielectr Electr Insul 14(1):146–155
101. Okabe S (2007) Evaluation of breakdown characteristics of oil-immersed transformers under non-standard lightning impulse - insulation characteristics for non-standard lightning impulse waveforms with oscillations. IEEE Trans Dielectr Electr Insul 14(3):679–688
102. Mitra P, De A, Chakrabarty A (2009) Investigation on the voltage stresses developed on transformer insulation under non-standard terminal excitations. In: Proc IEEE Region 10 Conf (TENCON) (2009). pp 1–5

103. Okabe S, Tsuboi T, Takami J (2009) Evaluation of k-factor based on insulation characteristics under non-standard lightning impulse waveforms. IEEE Trans Dielectr Electr Insul 16(4):1124–1126
104. Wang Z et al (2013) The oil-paper insulation breakdown characteristics under non-standard lightning impulse voltages. In: Proc IEEE Annual Report Electr Insul Dielectr Phenomena Conf (2013) pp 883–886
105. Krithika G, Usa S (2013) Volt-time characteristics of OIP under non-standard impulses. In: IEEE Condition Assessment Techniques In Electr Syst 1st Int Conf (2013). pp 281–285
106. Sankarganesh A, Karthikeyan K, Sudha R (2013) Breakdown characteristics of transformer under non-standard impulse voltage. Int J Eng Res Tech (IJERT) 2(4):1266–1269
107. Sarathi R et al (2013) Understanding the breakdown characteristics of liquid nitrogen under non-standard transient voltages. In: IEEE Industry Info Syst 8th Int Conf (ICIIS) (2013). pp 96–99
108. Sun P et al (2015) Study on voltage-number characteristics of transformer insulation under transformer invading non-standard lightning impulses. IEEE Trans Dielectr Electr Insul 22(6):3582–3591
109. Wang T et al (2015) Turn-to-turn insulation breakdown characteristics under non-standard lightning impulse voltages. In: Proc IEEE Prop App Dielectr Materials (ICPADM) 11th Int Conf (2015). pp 200–203
110. Wang Z et al (2015) Breakdown characteristics of oil-paper insulation under lightning impulse waveforms with oscillations. IEEE Trans Dielectr Electr Insul 22(5):2620–2627
111. Hua J et al (2017) Study on voltage-number characteristics of capacitor insulation under impulse voltages with different waveforms. In: IEEE 19th Int Conf Dielectr Liquids (ICDL) (2017). pp 1–4
112. Zhou Y et al (2017) Adjustment of wave front time and overshoot in lightning impulse test for transformer insulation. In: 2017 IEEE conference on electrical insulation and dielectric phenomenon (CEIDP) (2017). pp 270–273
113. Mubarak ZA, Usa S (2019) Effect of oil impregnated paper thickness and impulse waveshapes on voltage-number characteristics. Electr Eng (Springer) 101:1189–1197
114. Florkowski M et al (2020) Propagation of lightning, oscillating and non-standard impulse waveforms in transformer windings. In: Proc of the 21st international symposium on high voltage engineering (2020). pp 1254–1264. [Online]. Available: https://doi.org/10.1007/978-3-030-31676-1117